International Journal of Industrial Electronics, Control and Optimization © 2022 IECO
Vol. 5, No. 2, pp. 109-121, April 2022

Maximizing Electric Vehicles Owners Profit Considering Optimal Charging and Discharging Management in Distribution Networks Using Dynamic Programming

Ali Masoudi[1], Mohsen Simab[2,†], Hamidreza Akbari[3], Seyed Amin Saeed[4] , Tahereh Daemi[5]

[1, 3, 4, 5] Department of Electrical Engineering, Yazd branch, Islamic Azad University, Yazd, Iran
[2,†] Department of Electrical Engineering, Islamic Azad University, Marvdasht branch, Marvdasht, Iran

ABSTRACT

With an increasing penetration rate of electric vehicles in distribution networks, it is becoming vital to schedule their battery charging/discharging to maintain the network balance and increase the vehicle owners' profit. Electric vehicles are now considered one of the most important and accessible sources of revenue for their owners since they can be connected to the grid (V2G) as a power source during peak hours. As such, while flattening the power profile, they can improve the voltage drop across the grid buses. If charging/discharging of the vehicles is scheduled irregularly, the power drawn from the phases will become unbalanced, which can cause global outages and impair system stability in addition to increasing the harmonic volume and decreasing power quality. The present paper uses dynamic programming to reduce operating costs and enhance the profits of vehicle owners who participate in the V2G program. This optimization algorithm eliminates the undesirable paths leading to unconventional responses in the search space, which will greatly increase the speed and accuracy by which the optimal response is achieved. This model, along with multi-part tariffs on electricity prices, can lead to the more active participation of vehicle owners and help improve the power quality indices of the electrical parameters of the grid. The proposed method is simulated on a sample distribution network, and the case studies conducted prove the validity of the proposed algorithm.

Article Info

Research Article

Keywords:

Dynamic programming, Electric Vehicles, Optimization, Unbalancing

Article History:

Received 2021-10-13

Accepted 2022-02-24

I. INTRODUCTION

Nowadays, the widespread entry of electric vehicles (EVs) into the market has created an inseparable link between the two industries of electricity and transportation. The electricity industry must be prepared enough to embrace such changes from now on – changes that can either turn into a challenge for the electricity industry, in case of mismanagement and improper planning, or an opportunity, if a proper implementation framework is in place. The concept, which is interpreted as connecting the vehicle to the grid or V2G in short in today's scientific literature, is nothing but a win-win collaboration between the field of transportation and electricity supply, the optimal implementation of which requires to embed a new piece called electric vehicles in the complicated puzzle of the electricity industry [1-2]. EVs can store electricity in their batteries during off-peak hours when electricity is cheap and deliver it to the grid during peak hours when electricity prices are high. When looking at EVs parked and connected to the grid as sources of service, one enters into the V2G discussion [3]. In other words, V2G means using the battery capacity of EVs as an electric energy saver to provide electrical power or ancillary services to the power grid. Moreover, one of the other relevant parameters of

[†]**Corresponding Author:** msimab@miau.ac.ir
Tel: +98-7143311150, Faculty of Electrical and Computer Engineering, Islamic Azad University, Marvdasht branch, Marvdasht, Iran

Copyright © 2022 Simab et al. Published by University of Sistan and Baluchestan. This work is licensed under a Creative Commons Attribution-Noncommercial 4.0 International license. (https://creativecommons.org/licenses/by-nc/4.0/). Non-commercial uses of the work are permitted, provided the original work is properly cited

V2G is the control of the state of charge (SOC), whose impact on vehicle load management is examined here.

In addition to participating in electricity markets, V2G can also be used to play a complementary role in production from renewable resources. This means that fluctuations in the output power of power generation units such as wind and photovoltaic can be compensated by energy storage in batteries of EVs. The V2G required to stabilize solar power for peak power and wind power for base load is calculated in [4]. According to [5], four V2G-related markets include base load, peak, spinning reserve, and frequency regulation. The authors argue that V2G is unsuitable for base load, but it can be used for peak under certain conditions. It is competitive for the spinning reserve and highly competitive for regulation purposes. In the view of [6], V2G has two types, one-way and two-way. In the one-way type, the power direction is always from the grid to the vehicle, but in the two-way type, it is possible to inject the vehicle power into the grid. In other studies such as [7], V2G only refers to the second type, and the first type is called G2V.

The participation mode suggested by [8] for EVs in the electricity market in the V2G discussion is in such a way that EVs are in the charging phase at non-peak times, e.g., at night, and their aggregator contributes to amending the load curve. During the day and when the vehicles are parked, their aggregator can participate as a source in the regulatory market and can also be applied to reduce the peak. Reference [9] has studied the suitability of EVs for different markets in California and presented Table 1 in this regard. The applications mentioned for V2G in [9] include smoothing the power produced by wind farms and promoting short-term voltage stability.

TABLE I
VEHICLE OWNER'S POTENTIAL ANNUAL NET PROFIT FROM V2G IN CALIFORNIA ($) [1]

	Peak power ($)	Spinning reserve ($)	Frequency Regulation ($)
Battery Electric Vehicle	267	720	3162
Fuel Cell Electric Vehicle	-50 loss to 1226	2430 to 2685	2984 to 811
Hybrid Electric Vehicle	322	1581	-759 loss

Reference [10] has also emphasized the utilization of EVs and V2G to enhance the use of wind energy and has argued that the electricity, transportation, and heating industries can be scheduled in an integrated manner. According to the International Energy Agency, published in 2019, over the next 25 years, global energy demand will grow by 80%. A significant part of this energy is consumed in transportation, which is, on the other hand, one of the most important sources of production and emission of greenhouse gases [11]. One way to reduce the negative impact of battery charging on these vehicles is to manage their charging so that they are not charged simultaneously. Therefore, this reference has conducted research indicating that the peaks and valleys of the power curve can be flattened according to the habits of the American people in using their EVs. Studies on drivers' behavior have shown that their vehicles are parked for about 22 hours a day [12]. The energy in the batteries of EVs remains unused during this long parking time, so if they can be connected to the grid in a V2G manner, the energy stored in their batteries can be used to provide ancillary services, such as reducing peak power and spinning reserve [13].

The problems caused by the increased penetration rate of EVs in the grid are mostly related to the lack of control over the charger power of EVs and the lack of proper coordination between vehicles. Various research studies have been conducted on the regulation of EVs to adjust grid load, which are reviewed below. To increase the penetration factor of EVs, the starting time of the vehicle battery charging to the grid low-load intervals is shifted in [14]. To do this, it is assumed that there is a smart context between the grid and the vehicles in which the vehicles are aware of the energy price of the grid at any given time (Fig. 1). Vehicle owners also decide to charge their vehicle battery in less expensive hours. The grid can also prevent vehicle batteries from being charged during the network's peak load period.

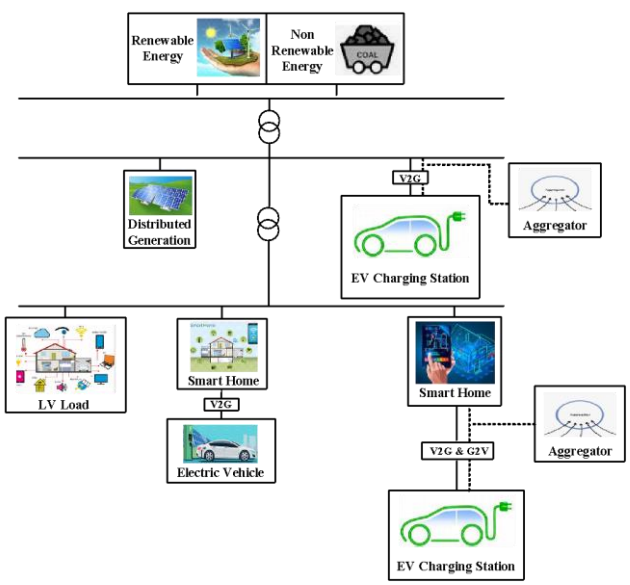


Fig. 1: The structure of a microgrid equipped with renewable resources and EV charging stations.

In addition to charging the batteries, the battery discharging state is also considered in [15] so that if the

vehicles connected to the grid have some energy in their batteries at the moment of connection, some vehicles can supply a part of their energy through the above-mentioned vehicles, which will ultimately reduce the energy loss. In this reference, the charging time of most vehicles is shifted to the lower load intervals. In [16], the optimal charging time of vehicles is obtained according to the grid load conditions and voltage profile, and the charging of vehicles is shifted to the low-load intervals of the grid. In this reference, in addition to determining the starting point of charging, the battery charging power is also controlled. In [17], a real-time load regulation method is presented in which EVs are charged in compliance with the priority of other vehicles at any time step. These studies have been carried out to solve the problems of increased energy demand in the grid peak load, for which the charging time of vehicles is generally shifted to the grid low-load intervals.

The present paper proposes a method based on dynamic programing that, in addition to a higher speed in finding the optimal response for battery scheduling of EVs, can identify insignificant paths during optimization and be careful not to pass them. Therefore, multi-stage dynamic programing is transformed into dynamic programing with a progressive approach in which the ways to reach from the zero stage to the final stage are modeled according to the vehicle battery charging state. Therefore, many non-optimal responses that are clearly identified before solving are removed from the search space, and the set of possible responses turns into a much smaller and convex space.

II. Optimal Charging and Discharging Formulation

The problem of charging several EVs in the grid, along with its technical and economic constraints, leads to the optimization of the following function:

$$cost(x^1, x^2, \dots, x^J) \quad ; \quad x^i \epsilon \theta^i \quad i = \{1, 2, \dots, N\} \tag{1}$$

where *cost (x)* is an objective function encompassing the power consumption parameters of the electric vehicle N in conditions *ix*. The power consumption or injection function of PEVs is defined by vector (2).

$$x^i = \left[x_1^i, x_2^i, \dots, x_k^i, \dots, x_{K^i}^i\right] \tag{2}$$

Set θi also defines all possible consumption or power injection modes for the 1st vehicle according to the following constraints. Given that the charger type is also important in this problem, regardless of its technology, the range of power exchanged between the PEV and the grid can be expressed by equation (3).

$$-\underline{p}^i < x_k^i < \underline{p}^i \quad \forall k \epsilon \{1, \dots, K^i\}, \forall i \epsilon \{1, 2, \dots, J\} \tag{3}$$

where $\underline{p}^i$ is the maximum nominal power of the charger used. The battery charging state must always remain within the permissible operating range. So, we will have:

$$\underline{SOC}^i < SOC_0^i + \tau \sum_{r=1}^{k} x_r^i < \underline{SOC}^i \tag{4}$$

τ is the length of the time steps and $\underline{SOC}^i$ and $\underline{SOC}^i$ are the minimum and maximum SOC, respectively. Therefore, the desirable SOC can be calculated by Equation (5), which is the same as the final charging of the vehicle battery. Of course, Equation (6) can also complement the formulation of the problem in cases where the charger type is not known.

$$SOC_{desired}^i = SOC_0^i + \tau \sum_{r=1}^{k} x_r^i \quad \forall i \epsilon \{1, 2, \dots, J\} \tag{5}$$

$$SOC_{desired}^i \leq SOC_0^i + \tau \sum_{r=1}^{k} x_r^i \leq SOC \tag{6}$$

III. Problem Solving by Dynamic Programing

In mathematics and optimization science, dynamic programing is an efficient way to solve a set of problems using the two characteristics of overlapping and optimal infrastructure sub-problems. In this method, like the division and solution method, the main problem is solved by combining the answers of the sub-problems, but the difference between the two methods is that in the division and solution method, the target problem is divided into a number of independent sub-problems and each one is solved separately. In the end, the answers are combined. But, in dynamic programing, the problems should not be completely independent, meaning that the sub-problems themselves have common constraints. These common sub-problems, although derived from separate paths, have the same answer in both cases and do not need to be recalculated. Therefore, in dynamic programing, the answers to these sub-problems are stored in a table or matrix so that they can be re-accessed. This difference may seem very simple and negligible, but in practice, problem-solving time is significantly reduced with this very simple solution. In general, problem-solving by the dynamic programing method is very similar to the inductive problem-solving method because, just like induction, in dynamic programing, the problem is divided into smaller problems but similar to the main problem, and the answer to the main problem is obtained by assuming the answer to these smaller problems. Finally, a step must be achieved whose answer could be easily calculated although a kind of induction is usually used to prove its accuracy. Dynamic programing is commonly applied to solve optimization and counting problems, including the arrival and departure times of EVs. The general model of the system under optimization is expressed using equation (7):

$$x_{k+1} = f_k(x_k, u_k, \xi_k) \quad k = 0, 1, \dots, T-1 \tag{7}$$

where k is a discrete interval time and f_k is a function that represents the model of the whole system. It models the state of the system in interval k, and u_k also shows the control and decision-making of system variables in passing from x_k to x_{k+1}. Furthermore, parameter ξ_k represents a random variable used for optimization. Therefore, the predicted value of the function with respect to the combined random variables included in the income function can be represented using equation (8).

$$Z = E\left(\sum_{k=0}^{T-1} \Phi(x_k, u_k, \xi_k) + \Phi_T(x_k)\right) \tag{8}$$

where E represents the mean or expectation function and Φ models the target cost function in interval k, which depends on the system state and the random variable. Using the control law of acceptable paths, ψ can be defined to be a mapping from x_k to u_k, in such a way that:

$$\psi = \{\Omega_0, \Omega_1, \dots, \Omega_{T-1}\} \quad \Omega_k(x_k) = u_k \tag{9}$$

$$u_k \in \Gamma_k(x_k) \subset \hat{\Gamma}_k \tag{10}$$

The set Γ_k includes all possible states for decisions of the control variable in interval k, and $\Gamma_k(x_k)$ is a non-empty subset of Γ_k that depends on the current state of the system. Therefore, we will have $x_k \in \Pi_k$ where the set Π_k contains all the states of the system in interval k.

Assume that the initial state of the system x_0 and the initial conditions of the control law, i.e. $\psi = \{\Omega_0, \Omega_1, \dots, \Omega_{N-1}\}$, exist, so the expected final cost of the system will be:

$$Z_\psi(x_0) = E\left(\sum_{k=0}^{T-1} \Phi(x_k, \Omega_k(x_k), \xi_k) + \Phi_T(x_k)\right) \tag{11}$$

where N is a set of acceptable paths in control theory. Therefore, the final function under optimization can be defined as follows:

$$Z_{\psi^*}(x_0) = Z^*(x_0) = \{Z_\psi(x_0)\} \tag{12}$$

where $\psi*$ is the optimal control and $Z^*(x_0)$ denotes its optimal cost.

Fig. 2 illustrates a dynamic programing problem-solving diagram with a multi-step approach, while Fig. 3 shows dynamic programing with a progressive approach. The difference between the two approaches is that in multi-step methods, there is a path from all nodes of the current stage to the nodes of the next stage, and this path includes all possible scenarios. This slows down the optimization performance. In dynamic programing with a progressive approach, it is possible to eliminate impossible states or states that clearly do not have the optimal response in those nodes (or paths) by using restrictive constraints that are applied to the system. Therefore, the routes passing from the current node to the next step node are not necessarily available.

To solve the problem of optimizing the charging and discharging time of EVs in the power grid, the most important parameter that is considered can be written, regardless of the system noise, as follows:

$$SOC_{k+1} = SOC_k + \Delta t\, p_k \tag{13}$$

The $\hat{\Gamma}_k$ set can be defined as the output powers of the batteries shown in equation (14).

$$-p_{max} < p_k < p_{max} \quad \forall\, k \epsilon \{0, 1, \dots, T-1\} \tag{14}$$

According to Fig. 4, to indicate how to optimize the charging/discharging schedule of vehicles using dynamic programing, the permissible interval of battery charging state is expressed by equation (15) as follows:

$$SOC_k^{min} < SOC_k < SOC_k^{max} \tag{15}$$

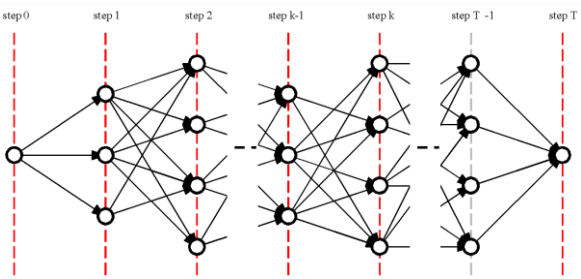


Fig. 2: Dynamic programing block diagram with a multi-stage approach.

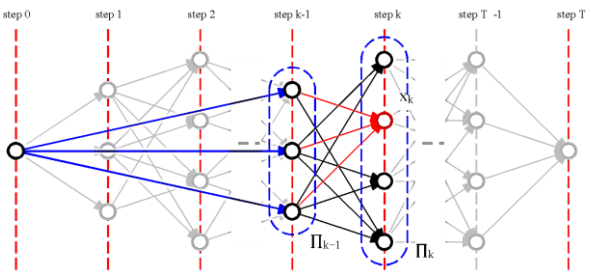


Fig. 3: Dynamic programing block diagram with a progressive approach.

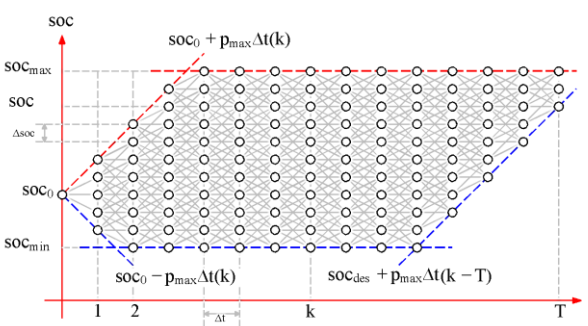


Fig. 4: Dynamic programing diagram in optimizing battery charging/discharging.

The parameters SOC_k^{min} and SOC_k^{max} are defined in terms of k in the form of equations (16) and (17):

$$SOC_k^{min} = \{SOC^{min}, SOC_0 - P_{max}\Delta t(k), SOC_{desired} + p_{max}\Delta t(k-T)\} \quad (16)$$

$$SOC_k^{max} = \{SOC^{max}, SOC_0 + P_{max}\Delta t(k)\} \quad (17)$$

According to Fig. 4, it is noteworthy that SOC_k^{min} and SOC_k^{max} do not depend only on the upper and lower limits of the battery charging rate but also on the maximum power drawn from the battery for charging/discharging. On the other hand, we have $\Gamma_k(SOC_k) \subset \hat{\Gamma}_k$, which depends on the state variations of the SOC_k variable. Therefore, considering the application of the dynamic programing method in this problem, we will have the following equation for the time $k-1$.

$$\frac{SOC_k - SOC_k^{max}}{\Delta t} < p_{k-1} < \frac{SOC_k - SOC_k^{min}}{\Delta t} \quad (18)$$

Then, the diagram block presented in Fig. 4 should be updated to Fig. 5 to achieve the progressive state.

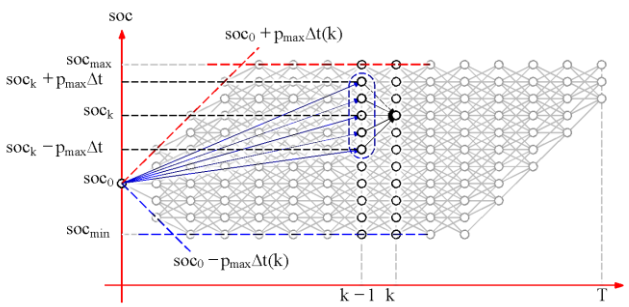


Fig. 5: Dynamic programing diagram with a progressive approach.

IV. Solution Algorithm

If the generating capacity of the vehicles directed towards the power aggregator is introduced using equation (19), then the total cost function can be approximated based on the grid load by equation (20).

$$P^i = [p_1^i, p_2^i, \dots, p_k^i, \dots, p_T^i] \quad (19)$$

$$G_i(P^i, P^{-i}) = -\sum_{k=1}^{T}\left(\left(p_k^i + \sum_{j=1, j\neq i}^{N}(p_k^j + l_k)\right) - L_{mean}\right)^2 \quad (20)$$

where L_{mean} is the average grid load and determined using equation (21).

$$L_{man} = \frac{\frac{1}{\Delta t}\sum_{i=1}^{N}(SOC_{desired}^i - SOC_0^i) + \sum_{k=1}^{T} l_k}{T} \quad (21)$$

Moreover, the power set of each vehicle, as an important actor, in supplying the grid load will be:

$$P^{-i} = [P^1, P^2, \dots, P^{i-1}, P^{i+1}, \dots, P^N] \quad (22)$$

In order to simplify the cost function, we can write:

$$L_k^{-i} = -\sum_{j=1, j\neq i}^{N}(p_k^j - l_k) + L_{mean} \quad (23)$$

Which results in:

$$G_i(P^i, P^{-i}) = -\sum_{k=1}^{T}(p_k^i - L_k^{-i})^2 \quad (24)$$

The optimal power is denoted by P^{i*}. Fig. 6 displays the flowchart of the proposed optimization algorithm. Therefore, the general problem-solving process will be as follows. First, the grid information, including the balanced and unbalanced loads as well as the number of EVs in the grid, is identified. Also, the grid demand rate, the temporal priority of vehicle charging, the voltage range of grid feeders, etc. are defined as input variables at this stage.

In the next step, V2G and G2V algorithms are introduced to the vehicles so that each vehicle can determine how to enter and depart according to the price of upstream electricity. The information of each vehicle is then sent to the ISO.

Afterward, the SOC of each vehicle is evaluated. According to the dynamic programing method, if the SOC is less than the minimum or more than the maximum, the charging or discharging process is stopped, and the load limit for vehicles is set. According to the imbalance rate and grid losses, the distance that each vehicle can travel could be calculated.

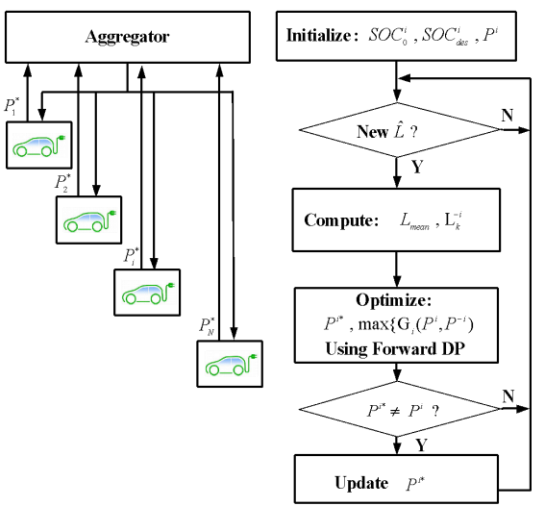


Fig.6: Optimization algorithm flowchart.

In the final stage, each vehicle that is connected to the upstream grid enters the load distribution, and the permissible ranges for the voltage of the feeders and the active and reactive power flowing on the grid lines are evaluated. This process is updated again after each vehicle is connected to or disconnected from the network. If the grid constraints are not observed during the G2V process, the vehicle connected to the grid and the other vehicles waiting to be charged will be shifted to the next interval.

Progressive load distribution methods have widely been used in distribution load calculations due to their high speed and little need for computer memory, as well as their good convergence characteristics. The general algorithm here

consists of two basic steps, including backward sweep and forward sweep, which are repeated until convergence is achieved. These methods are divided into three categories of sum current method, power sum method, and impedance sum method.

The general steps of the algorithm are as follows:

1) backward sweep: Starting from the end bus and moving towards the slack bus, the branch powers are calculated.

$$S_n = S_i + \sum_{m \epsilon M} S_m + Loss_n \quad (25)$$

where S_n is the branch power n, S_i indicates the power injected into the load connected to the node *i*, *M* is the sum of the branches connected to branch *n* in node *i*, S_m represents the power of branch *m* and $Loss_n$ is the losses of branch *n*, which are zero in the first iteration.

2) Forward sweep: Starting from the branches connected to the slack bus and moving towards the end branches, the currents in the bus of the sending branch n (j) and the voltages in the bus of the receiving branch (n), i, are calculated.

$$I_n = \left(\frac{S_n}{V^j}\right)^*$$
$$V^i = V^j - Z_n * I_n \quad (26)$$
$$Loss_n = -(V^i - V^j) * I_n^*$$

3) Voltage mismatch calculation: After the two above-mentioned steps were completed in each iteration, the voltage mismatch is calculated for all buses:

$$\Delta V^{i^{(k)}} = \left|V^{i^{(k)}}\right| - \left|V^{i^{(k-1)}}\right| \quad (27)$$

where k is the number of iterations. If each of the ΔV_i values is greater than the convergence criterion, steps 1 and 2 are repeated until convergence is achieved.

EV units that are included in the model as a PQ bus in the form of a negative load are controlled. That is, it is enough to reduce the amount of active and reactive power produced by the EV from the power consumption of the bus and do the load distribution. However, to include the distributed production units that are controlled as a PV bus, additional processes are needed to solve the load distribution. A compensation technique is used to control PV nodes. The basic idea of this method is that in order to obtain the voltage in a PV node, it is necessary to determine the correct amount of reactive current injection generated by the unit. For this purpose, in each PV bus, the constants for the generator are determined, i.e., the actual power output (P) and the voltage range (V). Then, this bus is considered a PQ bus in the load distribution algorithm. After the load distribution is converged, the optimal response is achieved using the voltage control sensitivity matrix and the reactive power control constraint in the PV bus.

The voltage variance index, which is known to indicate the improvement of the voltage profile, will also, be equal to:

$$f_v = \sum_{ni=1}^{n_n} (V_{ni} - V_{rated})^2 \quad (28)$$

Also for the voltage stability index we have:

$$SI_{(n_i)} = |V_{mi}|^4 - 4[P_{ni}(ni)R_{ni} + Q_{ni}(ni)X_{ni}]|V_{mi}|^2 - 4[P_{ni}(ni)R_{ni} + Q_{ni}(ni)X_{ni}]^2 \quad (29)$$

In addition, for the (current) load balance index we have:

$$f_{unbl} = \sum_{i=1}^{m} \left(\frac{I_{ni}}{I_{nj\cdot avg}}\right)^2 \quad (30)$$

$$I_{nj.avg} = \frac{1}{m}\sum_{j=1}^{m} I_{nj} \quad (31)$$

In which the current I_{ni} must always be close to I_{nj} so that the imbalance is eliminated.

V. Simulation

In order to validate the proposed method, three different case studies are presented in this paper, which are described below.

A. Case Study 1

In this case study, it is assumed that the electricity tariff is two-part, so the profit from the sale of battery power to the grid in the V2G state is directly related to the amount of charge in the batteries. It is assumed that four EVs shown in Fig. 7 are connected to the network and to buses 2, 4, 5, and 8. The initial charge of the batteries, their capacity, and other vehicle specifications are presented in Table (2).

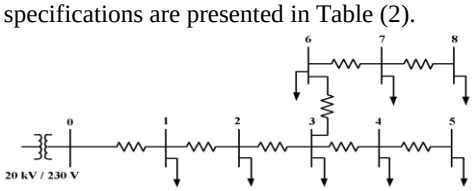


Fig. 7: Distribution grid considered in the case study 1.

Table II

CHARACTERISTICS OF THE MICROGRID IN CASE STUDY 1

Parameter	Value
Effective system voltage	230 (rms)
Line frequency	50 Hz
No. of connected buses	(5, 8, 4,2)
Battery capacity	(15, 15,16,20) kWh
Initial charge rate	(5, 8,3/2, 6/4) kWh
Final charge rate	(12, 15,15,17) kWh

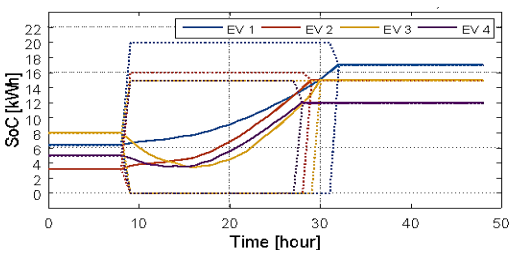
As shown in Figures 8(a) and (b), the load profile becomes flatter when the vehicles are discharged. Since the single-part tariff has been considered to be 2 USD/kWh during all hours of the day, the payment cost will be:

$$cost_{single\ tarrif} = \sum_{j=1}^{N_{car}} P^j \times \pi^j \qquad (32)$$

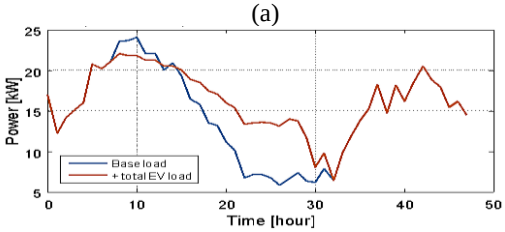
According to the diagram and after simplification, we will have:

$$cost_{single\ tarrif} = 36.40^{kWh} \times 2^{\$/kWh} = 72.8\ \$ \qquad (33)$$

Figures 9(a) and (b) also illustrate the diagrams of voltage-bus profiles of the grid and battery output power of vehicles, respectively. In the two-part tariff, we consider the price of electricity at 15 to 33 hours to be \$2.8 and at the remaining hours to be \$2. In this case, the amount paid to the distribution company is equal to \$54.72 according to the diagrams in Fig. 10 and Equation (25), which has resulted in a saving of \$18.08. The amount of profit also increases correspondingly. The diagrams in Fig. 11 also show the voltage profile of the main buses and the output power of the vehicle batteries. Compared to the single-part tariff, it can be seen that the bus voltages have been improved.

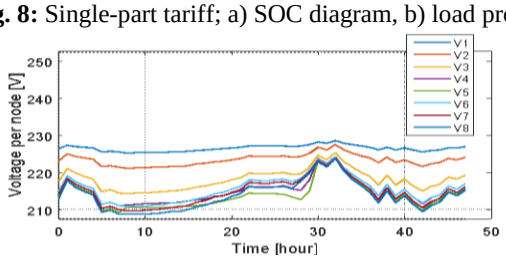


(a)

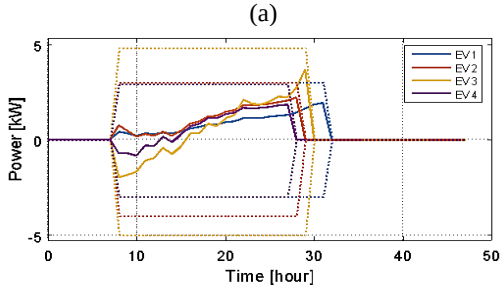


(b)

Fig. 8: Single-part tariff; a) SOC diagram, b) load profile

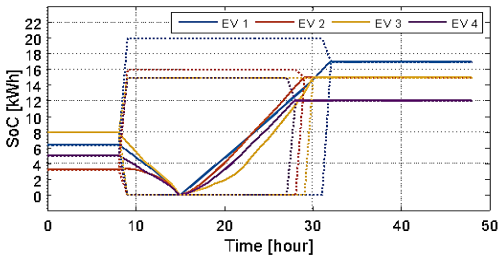


(a)

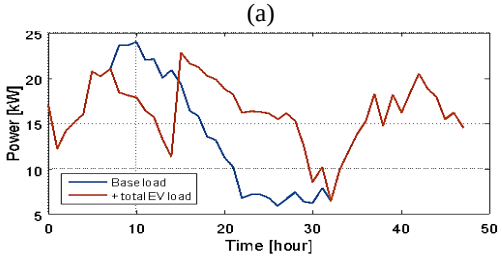


(b)

Fig. 9: Single-part tariff; a) Voltage profile, b) Battery output power

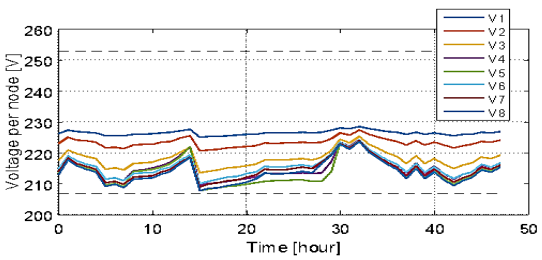


(a)

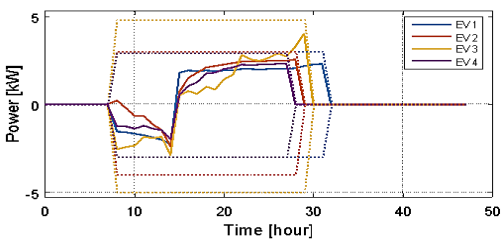


(b)

Fig. 10: Two-part tariff; a) SOC diagram, b) load profile



(a)



(b)

Fig. 11: Two-part tariff; a) Voltage profile, b) Output power of batteries

B. Case Study 2

In order to investigate the imbalance in the distribution network and to see how to balance it by the optimal management of vehicle battery charging/discharging, the power drawn from all three phases of the distribution system is investigated in this case study. Since the distribution systems in different feeders might be unbalanced and this imbalance may disturb the load balance, this study assumes that the power required for each vehicle battery is unequal (which is, of course, the case in practice) [18]. If the imbalance index of the main voltage is defined by equation (34), it is possible to drastically reduce the amount of imbalance by introducing a conversion function (35) so that the voltage of the negative and positive sequences gets very close to each other.

$$V_{unb} = \left|\frac{V^{-}_{PEV,k}}{V^{+}_{PEV,k}}\right| * 100 \quad (34)$$

$$OF = \{(V_{unb})\} \quad (35)$$

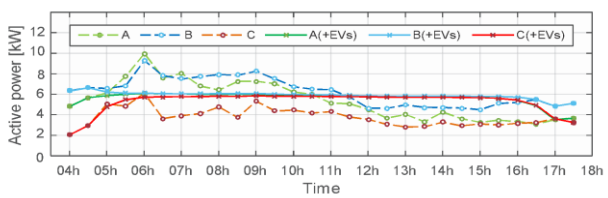
where parameters $V^{-}_{PEV,k}$ and $V^{+}_{PEV,k}$ are introduced by equations (36) and (37), respectively.

$$V^{-}_{PEV,k} = \frac{1}{3}\left(V^{a}_{PEV,k} + \beta V^{b}_{PEV,k} + \beta^2 V^{c}_{PEV,k}\right) \quad (36)$$

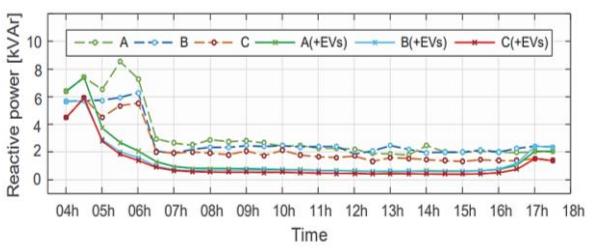
$$V^{+}_{PEV,k} = \frac{1}{3}\left(V^{a}_{PEV,k} + \beta \hat{} V^{b}_{PEV,k} + \beta V^{c}_{PEV,k}\right) \quad (37)$$

Parameter β is equal to $1\angle 2\pi 3$ which is extracted from the Fortescue matrix [19]. Considering the above equations and integrating them in the dynamic programing, the active and reactive power consumption of vehicles in each bus can be seen in the diagrams in Fig .12.

Before connecting the vehicles to the circuit, the imbalance in the power of all three phases is drawn with the lines, but with proper charging and discharging management of the vehicles (the dashed line), the imbalance is practically eliminated and the power of each of the three phases becomes roughly balanced [20]. The active and reactive diagrams drawn from all three phases are illustrated in Fig .12, in which they are shown with bold lines.



(a)



(b)

Fig. 12: Investigation of balancing the power drawn from all three phases in the distribution grid; a) Active power, b) Reactive power

C. *Case Study 3*

In this case study, it is assumed that five EVs are individually connected to the grid for six hours and charged. If the vehicles are connected to the grid irregularly, the diagram shown in Fig. 13 indicates that the load profile will also have large oscillations asymmetrically. This proves the importance of how the use of EVs is scheduled so that the load profile that is to be provided by the grid could exhibit the maximum flatness. The power consumption diagram of vehicles that are connected to the balanced distribution grid in a regular manner and with the same power is shown in Fig.14.

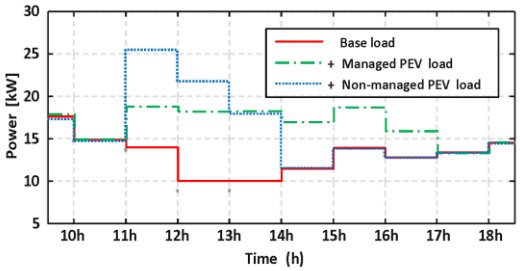


Fig. 13: Comparison of vehicle power consumption in managed/unmanaged charging states

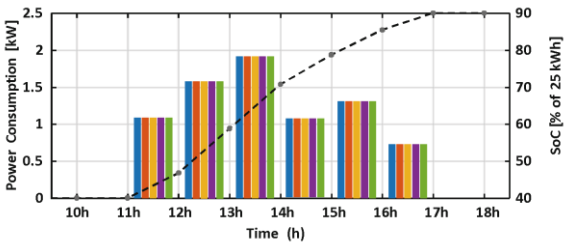


Fig. 14: Power consumption of each vehicle in the managed charging state with its SOC

D. *Case Study 4*

In this section, which is the continuation of the case study 3, it is assumed that the penetration rate of vehicles in the distribution grid is changed. Therefore, four different cases are evaluated below. It is noteworthy that the reliability indices have fully been described in [21-22].

1) The system without any vehicles

In this scenario, the grid is at a resting state and there is no PHEV. Therefore, active and reactive power control, as well as voltage and frequency rate control is performed only by the upstream operator, and consumers are not involved in the price. In this case, unsupplied energy may increase at peak load and reduce the grid reliability. Load response sources are not used here either.

2) PHEVs are on the grid but their charging is not managed:

In this scenario, the vehicles are connected to the grid, but their charging process is not managed, and each vehicle can get power from the grid at any time. This can cause a voltage drop at peak load because the vehicles are connected to the grid like extra loads in this scenario and the grid control is extremely difficult. This scenario shows the negative impact of using EVs.

3) Charging of PHEVs is managed (vehicles do not have returning storage source)

In this scenario, EVs are connected to the grid and are charged, but they do not deliver energy to the grid. Their only advantage for the grid is the reduction of pollutants and the reduction in the use of fossil fuels. In this case, the vehicles are charged in a managed manner (at low load) and are not connected to the grid during peak load.

4) Both managed charging and V2G scenario are applied (vehicles have returning storage source)

At this stage, in addition to the fact that charging of the vehicles is scheduled, the unused energy discharge of their batteries is also managed in the grid during production shortage. This scenario indicates the positive impact of using EVs.

5) Evaluation of Results

Comparing the results of cases 3 and 4 with case 2 shows that scheduled charging not only has a less negative effect than uncontrolled charging but also improves grid reliability. Unmanaged charging reduces reliability by 92%. PHEVs act as storage systems in the V2G state, thereby improving system reliability by 19%.

The results also suggest that the reliability indices are significantly affected by the unmanaged charge of PHEVs. Because the penetration of PHEVs into the smart grid is significantly increased, the grid reliability will sharply reduce if the proper charge management strategy is not implemented. In addition, the results show that the LOEE index (Loss of Energy Expected) is reduced by about 2.5% in the unmanaged charging state and also when charging the electric vehicle is only possible at home (during holidays). Using a managed charging strategy, especially in the V2G state and when charging scheduling is applied at home or work, the LOEE index is improved by about 2.92%. The results of comparing the above cases show that by implementing the proposed charge management methods, PHEV risks for grid reliability can be turned into an opportunity to improve it. With a managed charging strategy in case 3, the problems caused by load demand for charging PHEVs can be controlled. In the V2G strategy mentioned in case 4, the LOEE index and EENS (Energy Expected Not Supplied) are reduced compared to case 1 where there is no PHEV on the grid.

To evaluate the proper performance of the smart grid, the sensitivity analysis of important parameters such as charging level and penetration rate of PHEVs in the LOEE index was performed whose results are illustrated in Figures (15) to (17). These figures exhibit the changes in the LOEE index in relation to the level changes in charge and penetration rate of PHEVs in cases 2, 3, and 4. In the LOEE, sensitivity analysis was conducted for charging level factors (CLF) and PHEV penetration factors (PPF). CLF and PPF are multiplied by the current values of the charging level and the penetration level of electric vehicles, respectively. Then, the reliability indices are calculated, so it is possible to examine the importance of the charging level and the penetration level of PHEVs on the reliability parameters. The LOEE sensitivity in the unmanaged charging scenario for PPF and CLF changes is also shown in Fig.15.

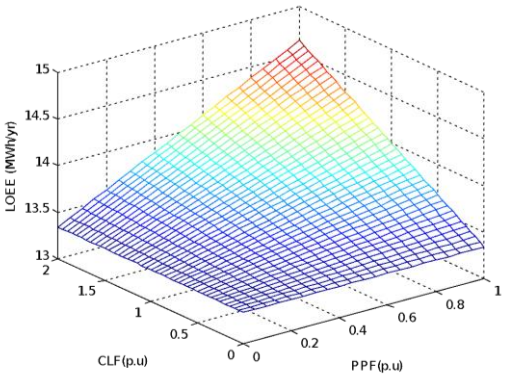


Fig. 15: LOEE index sensitivity based on CLF and PPF in the case 1.

As illustrated in Fig. 15, in the unmanaged charging scenario of PHEVs, as the penetration level of EVs (increased PPF) and their charging level (increased CLF) are increased, the LOEE index also rises. The system reliability decreases with an increase in the number of PHEVs whose charging has not been managed. The results also indicate that the charging level parameter increases the negative impacts of unmanaged charging of PHEVs. According to the results of sensitivity analysis, the worst grid reliability situation in the unmanaged charging of electric vehicles scenario occurs at the fast charging level and at maximum penetration of EVs. The results of case 1 (the scenario of unmanaged charging of EVs) suggest that changing the penetration of PHEVs and charging level have a similar effect. In electrical networks where it is not possible to use advanced communication and information technologies, the charging level of EVs can be reduced to improve system reliability. The LOEE changes in terms of large CLF changes and PPF (between 0 and 2) are shown in Fig. 16.

According to the results in Fig. 16, in the unmanaged charging scenario, when the EVs are charged with the maximum charging level, the grid reliability is drastically reduced. Fig. 16 shows the result of LOEE sensitivity analysis with respect to PPT and CLF changes in the V2G scenario. The load demand and production curves on a critical day in both the unmanaged charging scenario and the V2G scenario are compared. In the critical situation, the two main feeder transformers of the grid have been out of the circuit. In this situation, in the case of unmanaged charging, the load and production diagrams are shown in Fig. 17, and the load and production diagrams of an IEEE 34-bus grid in the V2G scenario are displayed in Fig. 18.

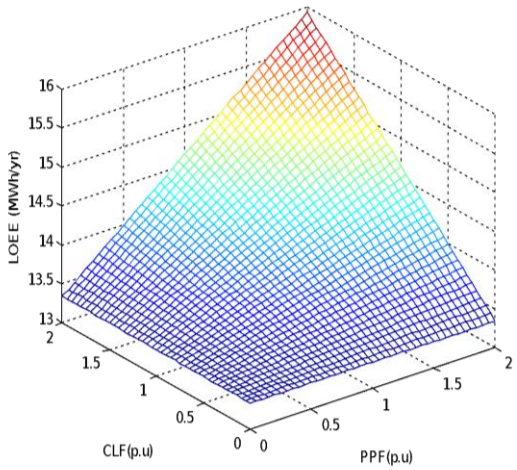


Fig. 16: Sensitivity of the LOEE index based on CLF and PPF in case 1 in a wide range of changes.

Therefore, it can be argued that the use of EVs can have favorable and unfavorable impacts on the grid, which requires strong management to operate it. In addition to increasing system losses, unmanaged vehicle charging also raises operating costs and reduces network reliability. SOC management is one of the most important operating parameters of the problem that can clearly affect network performance. Finally, Table (3) compares the proposed method with the existing methods. It is observed that in the proposed method, both the voltage imbalance index is lower than that of the other methods and the range of SOC changes is increased.

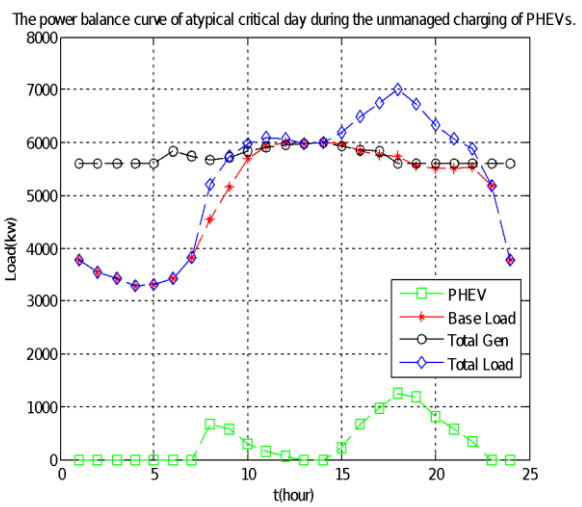


Fig. 17: Load supply in unmanaged charging state

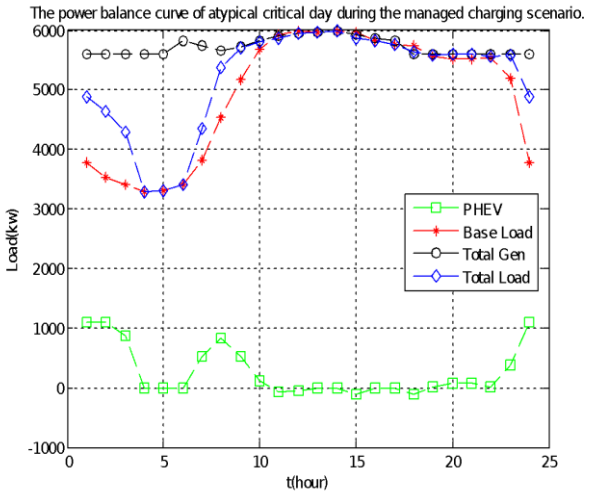


Fig. 18: Load supply in the managed charging state

Table III

COMPARISON OF THE PROPOSED METHOD WITH CONVENTIONAL METHODS

Method	Profit rate in scenario 1	SOC range	Voltage imbalance index
[5]	$ 16.236	(20-80)%	1.9%
[7]	$ 16.562	(20-85)%	1.8%
[17]	$ 18.105	(25-85)%	1.9%
Proposed method	$ 18.723	(15-90)%	1.5%

VI. CONCLUSION

In this paper, optimal scheduling to set the appropriate connecting time of EVs to a low-voltage distribution network has been presented. Since supplying peak load during peak for the distribution network is usually associated with many problems, EVs can help the network during these hours and flatten the load profile by injecting extra power.

According to the case studies conducted here, it is concluded that the two-price tariff benefits vehicle owners more and increases their participation in improving network voltage drops. An optimal vehicle charging and discharging schedule can also eliminate imbalances in the distribution network and act as reactive power control devices. When the charging/discharging of vehicles is not managed, fluctuations in the grid power profile increase, which can be considered a threat to grid security. Hence, all the problems mentioned can be reduced to a minimum level by using dynamic programming with a progressive approach.

TABLE IV
NOMENCLATURE

Variable	Explanations
x^i	Terms of operation EVs
θ^i	The set of all power injection or absorption by EVs
N	Number of EVs
i	EV number i
$\underline{p}$	Maximum Generation of EVs
SOC_0^i	Initial SOC
$\underline{SOC^i}$	Maximum SOC
$\underline{SOC^i}$	Minimum SOC
τ	Length of sampling time steps
$SOC_{desired}^i$	Desired SOC
f_k	The whole system modeling function
ξ_k	Positive random variable
$E(x)$	Mean function
Φ	Cost of f_k function
ψ	A mapping of x_k too u_k
$\hat{\Gamma}_k$	All the possible states for control variable decisions
$\Gamma_k(x_k)$	An non-empty subset of $\hat{\Gamma}_k$
Π_k	All the system states in k interval
Z	Expected value for the objective function
ψ^*	Optimal control
$Z^*(x_0)$	ψ^* cost
L_{mean}	Network average load
P^{i*}	Optimal powers
$V_{PEV,k}^-$	Negative sequence voltage of vehicles
$V_{PEV,k}^+$	Positive sequence voltage of vehicles
S_n	Power of branch *n*
S_i	Power injected to the bus *i*
M	set of branches connected to branch *n* in bus *i*
$Loss_n$	Losses of branch n
$P_{ni}(ni)$	Active power between n and i buses
$Q_{ni}(ni)$	Reactive power between n and i buses
R_{ni}	Line resistance between bus n and bust i
X_{ni}	Line reactance between bus n and bus i
I_{nj}	Current of the line between bus *n* and bus *i*
$I_{nj.avg}$	Average current of the line between bus *n* and bus *i*

REFERENCES

[1] R. Iacobucci, B. McLellan, and T. Tezuka, "Optimization of shared autonomous electric vehicles operations with charge scheduling and vehicle-to-grid," *Transportation Research Part C: Emerging Technologies*, vol. 100, pp. 34–52, Mar. 2019.

[2] H. Soltani Gohari, K. Abbaszadeh, and J. Gholami Gorji, "A Controllable Bidirectional Rectifier for EV Home Charging Station with G2H/G2VH/V2H/V2G Functions," *International Journal of Industrial Electronics Control and Optimization*, vol. 4, no. 1, pp. 99-113, 2021.

[3] M. Ramzanzadeh, M. Jafari Nokandi, T. Barforoushi, and J. Saebi, "Security-Constrained Unit Commitment in the Presence of Demand Response Programs and Electric Vehicles," *International Journal of Industrial Electronics Control and Optimization*, vol. 3, no. 3, pp. 313-326, 2020.

[4] L. Yao, Z. Damiran, and W. H. Lim, "Optimal Charging and Discharging Scheduling for Electric Vehicles in a Parking Station with Photovoltaic System and Energy Storage System," *Energies*, vol. 10, no. 4, p. 550, Apr. 2017.

[5] Y. Cao, L. Huang, Y. Li, K. Jermsittiparsert, H. Ahmadi-Nezamabad, and S. Nojavan, "Optimal scheduling of electric vehicles aggregator under market price uncertainty using robust optimization technique," *International Journal of Electrical Power & Energy Systems*, vol. 117, p. 105628, May 2020.

[6] Y. Zheng, S. Niu, Y. Shang, Z. Shao, and L. Jian, "Integrating plug-in electric vehicles into power grids: A comprehensive review on power interaction mode, scheduling methodology and mathematical foundation," *Renewable and Sustainable Energy Reviews*, vol. 112, no. 1, pp. 424-439, 2019.

[7] H. Ahmadi-Nezamabad, M. Zand, A. Alizadeh, M. Vosoogh, and S. Nojavan, "Multi-objective optimization based robust scheduling of electric vehicles aggregator," *Sustainable Cities and Society*, vol. 47, p. 101494, May 2019.

[8] A. Triviño-Cabrera, J. A. Aguado, and S. de la Torre, "Joint routing and scheduling for electric vehicles in smart grids with V2G," *Energy*, vol. 175, pp. 113–122, May 2019.

[9] C. Goebel and D. S. Callaway, "Using ICT-Controlled Plug-in Electric Vehicles to Supply Grid Regulation in California at Different Renewable Integration Levels," in *IEEE Transactions on Smart Grid*, vol. 4, no. 2, pp. 729-740, June 2013.

[10] Z. Wang, P. Jochem, and W. Fichtner, "A scenario-based stochastic optimization model for charging scheduling of electric vehicles under uncertainties of vehicle availability and charging demand," *Journal of*

Cleaner Production, vol. 254, p. 119886, May 2020.

[11] M.-W. Tian, S.-R. Yan, X.-X. Tian, M. Kazemi, S. Nojavan, and K. Jermsittiparsert, "Risk-involved stochastic scheduling of plug-in electric vehicles aggregator in day-ahead and reserve markets using downside risk constraints method," *Sustainable Cities and Society*, vol. 55, p. 102051, Apr. 2020.

[12] M. U. Javed, N. Javaid, A. Aldegheishem, N. Alrajeh, M. Tahir, and M. Ramzan, "Scheduling Charging of Electric Vehicles in a Secured Manner by Emphasizing Cost Minimization Using Blockchain Technology and IPFS," *Sustainability*, vol. 12, no. 12, p. 5151, Jun. 2020.

[13] A. González-Garrido, A. Thingvad, H. Gaztañaga, and M. Marinelli, "Full-scale electric vehicles penetration in the Danish Island of Bornholm—Optimal scheduling and battery degradation under driving constraints," *Journal of Energy Storage*, vol. 23, pp. 381–391, Jun. 2019.

[14] Y. Luo, G. Feng, S. Wan, S. Zhang, V. Li, and W. Kong, "Charging scheduling strategy for different electric vehicles with optimization for convenience of drivers, performance of transport system and distribution network," *Energy*, vol. 194, p. 116807, Mar. 2020.

[15] J. Su, T. T. Lie, and R. Zamora, "A rolling horizon scheduling of aggregated electric vehicles charging under the electricity exchange market," *Applied Energy*, vol. 275, p. 115406, Oct. 2020.

[16] E. Hadian, H. Akbari, M. Farzinfar, and S. Saeed, "Optimal Charging/Discharging Control of Electric Vehicle Charging Station Considering Grid Resiliency," *International Journal of Industrial Electronics Control and Optimization*, vol. 4, no. 4, pp. 453-464, 2021.

[17] S. Seyyedeh Barhagh, M. Abapour, and B. Mohammadi-Ivatloo, "Optimal scheduling of electric vehicles and photovoltaic systems in residential complexes under real-time pricing mechanism," *Journal of Cleaner Production*, vol. 246, p. 119041, Feb. 2020.

[18] C. Sabillon-Antunez, O. D. Melgar-Dominguez, J. F. Franco, M. Lavorato and M. J. Rider, "Volt-VAr Control and Energy Storage Device Operation to Improve the Electric Vehicle Charging Coordination in Unbalanced Distribution Networks," in *IEEE Transactions on Sustainable Energy*, vol. 8, no. 4, pp. 1560-1570, Oct. 2017.

[19] M. R. Islam, H. Lu, M. J. Hossain, and L. Li, "Mitigating unbalance using distributed network reconfiguration techniques in distributed power generation grids with services for electric vehicles: A review," *Journal of Cleaner Production*, vol. 239, p. 117932, Dec. 2019.

[20] A. HossienPour, and A. Khajeh, "Determining Optimal Value of Pole Arc to Pole Pitch Ratio in order to Increasing Average Torque and Decreasing Unbalance Magnetic Force in Hybrid Electrical Vehicle, " *International Journal of Industrial Electronics Control and Optimization*, vol. 4, no. 4, pp. 445-451, 2021.

[21] C. Singh, Panida Jirutitijaroen, and J. Mitra, *Electric power grid reliability evaluation : models and methods*. Chichester: Wiley Blackwell, 2019.

[22] B. W. Tuinema, *Probabilistic reliability analysis of power systems : a student's introduction*. Cham, Switzerland Springer, 2020.



Ali Masoudi was born at Eqlid, Iran, at 1974. He received the B.sc. degree at electrical engineering at Islamic Azad University, Khomeyni Shahr Branch, Khomeyni Shahr, Iran at 2009 and the M.sc. at Islamic Azad University, Mehriz Branch Mehriz, Iran at 2015. He is currently working towards his PhD degree in the Islamic Azad University, Yazd Branch. Yazd, Iran. He is currently working as Exploitation Manager at Fars Electricity Distribution Company, Shiraz, Iran since 2000. His main research interests include analysis and design of electrical machines, power electronics and renewable energies.



Mohsen Simab received his BSc degree in Electrical Engineering from Amir Kabir University, Tehran, Iran in 2003 and obtained the MSc and PhD degrees from Tarbiat Modares University, Tehran, Iran, 2005, and 2011, respectively. He is an Assistant Professor in power systems at the Department of Electrical Engineering, Marvdasht Branch, Islamic Azad University, Marvdasht, Iran. His main research interests are electric distribution regulation, power system operation, and power system reliability.



HamidReza Akbari was born in Yazd, Iran, in 1980. He received the B.Sc. and M.Sc. degrees in electrical engineering from the Amirkabir University of Technology, Tehran, Iran, in 2001 and 2004, respectively, and the Ph.D. degree in electrical engineering from Islamic Azad University, Science and Research Branch, Tehran, in 2011. He is currently working as an Assistant Professor of Electrical Engineering with Islamic Azad University, Yazd Branch. His main research interests include analysis and design of electrical machines, power electronics and renewable energies.



Seyed Amin Saied received the M.Sc. and Ph.D. degrees in electrical engineering from the K. N. Toosi University of Technology, Tehran, Iran, in 2006 and 2012, respectively. He is currently with the Department of Electrical Engineering, Yazd Branch, Islamic Azad University, Yazd, Iran. His main research interests include the design and modeling of electrical machines, and electrical parameter estimation of electrical machines.



Tahere Daemi was born in Iran, in 1979. She received the B.Sc degree in 2002 from Yazd university, the M.S degree in 2005 Shiraz University and Ph.D degree in 2012 from Isfahan University of Technology. Currently, she is an Assistant Professor of electrical engineering department in Islamic Azad University, Yazd Branch, Iran. Her major field of study is reliability and security analysis, renewable energy resources, energy management with application of data mining and Bayesian Networks in power systems.

IECO

This page intentionally left blank.